0026-895X/96/051401-12$3.00/0

MOLECULAR PHARMACOLOGY, 50:1401–1412 (1996).

Dose-Response Relations for Unnatural Amino Acids at the Agonist Binding Site of the Nicotinic Acetylcholine Receptor: Tests with Novel Side Chains and with Several Agonists

PATRICK C. KEARNEY, MARK W. NOWAK, WENGE ZHONG, SCOTT K. SILVERMAN, HENRY A. LESTER, and DENNIS A. DOUGHERTY

Division of Biology (P.C.K., M.W.N., H.A.L.) and Division of Chemistry and Chemical Engineering (W.Z., S.K.S., D.A.D.), California Institute of Technology, Pasadena, California 91125

Received June 10, 1996; Accepted August 3, 1996

SUMMARY

Structure-function relations in the nicotinic acetylcholine receptor are probed using a recently developed method based on chemical synthesis of nonsense suppressor tRNAs with unnatural amino acid residues, site-directed incorporation at nonsense codons in *Xenopus laevis* oocytes, and electrophysiological measurements. A broad range of unnatural amino acids, as many as 14 at a given site, are incorporated at three sites, α93, α190, and α198, all of which are tyrosine in the wild-type receptor and are thought to contribute to the agonist binding site. Confirming and expanding upon earlier studies using conventional mutagenesis, the three tyrosines are shown to be in substantially different structural microenvironments. In particular, a crucial role is established for the hydroxyl group of αTyr93, whereas a variety of substituents are functional at the analogous position of αTyr198. Interestingly, consideration of three different agonists (acetylcholine, nicotine, and tetramethylammonium) does not discriminate between these two best-characterized binding site residues. In addition, double-mutation studies establish the independent effects of mutations at the pore region (second transmembrane region) and at the agonist binding site, and this observation leads to a novel strategy for adjusting EC_{50} values. These results establish the broad generality and great potential of the unnatural amino acid methodology for illuminating subtle structural distinctions in neuroreceptors and related integral membrane proteins.

This paper studies structure-function relations at an ion channel, using a recently developed (1) method based on chemical synthesis of nonsense suppressor tRNAs with unnatural amino acid residues (2), site-directed incorporation at nonsense codons in *Xenopus laevis* oocytes, and electrophysiological measurements. To the extent that this methodology is broadly applicable, it has the potential to provide new types of structural information about ion channels, receptors, and transporters. For example, biophysical probes, cross-linking agents, and tethered functionalities could be introduced in a site-specific, minimally perturbing way (3).

We study the mouse muscle nAChR (4–6), a relatively well understood ion channel with the stoichiometry $\alpha_2\beta\gamma\delta$; the agonist is thought to bind at the α subunits, possibly at the interfaces between the α/γ and α/δ subunits. We describe here the incorporation of a broad range of unnatural amino acids, as many as 14 at a given site. The consequences of these structural perturbations are evaluated by electrophysiological methods, using ACh and other agonists. The results establish that unnatural amino acid incorporation can be generally and efficiently used to probe structural issues in a functional region of a neuroreceptor. They also provide new insights into the possible roles of critical residues of the nAChR.

We also describe an additional strategy for structure-function studies of the nAChR. We have established that mutations in the M2 region that are known to lower EC_{50} values (7) act independently of structural changes at the agonist binding site. These M2 region mutations can thus be used to fine-tune EC_{50} values, to bring them into experimentally optimal ranges.

Concerning the nAChR, one intriguing and much discussed feature of the structure is the large number of aromatic residues (tyrosine and tryptophan) that have been located at the agonist binding site through affinity labeling and mutagenesis studies. Many aromatic amino acids are involved in

This work was supported by the National Institutes of Health (Grants NS34407 and NS11756) and by the Beckman Institute at Caltech.

ABBREVIATIONS: nAChR, nicotinic acetylcholine receptor; ACh, acetylcholine; TMA, tetramethylammonium; DOPA, 3,4-dihydroxyphenylalanine; NVOC, nitroveratryloxycarbonyl; THF, tetrahydrofuran; HEPES, 4-(2-hydroxyethyl)-1-piperazineethanesulfonic acid; M2, second transmembrane; DCI, direct chemical ionization; FAB, fast-atom bombardment; ESI, electrospray ionization; HRMS, high-resolution mass spectrometry; MS, mass spectrometry; DMF, dimethylformamide; DMSO, dimethylsulfoxide; MeOH, methanol; TFA, trifluoroacetic acid.

the only natural binding site for ACh with a known structure, acetylcholinesterase (8, 9). Whereas one can anticipate many possible roles for aromatic residues in defining a binding site, in acetylcholinesterase there is clear evidence for cation-π interactions in the binding of ACh, as discussed earlier (10, 11). The positively charged quaternary ammonium group of ACh interacts directly with the indole ring of a tryptophan of the esterase (9). In the nAChR, however, the presence of a tyrosine or tryptophan near the agonist binding site does not prove its involvement in cation-π interactions. In fact, it is not possible for all of the aromatic residues to directly contact the quaternary ammonium cation of ACh, and it remains an open question which, if any, of the aromatic residues involved in the agonist binding site of the nAChR undergo direct cation-π interactions with the agonist.

We considered that the unnatural amino acid methodology might be able to distinguish the various roles played by the many aromatic residues at the agonist binding site. Considering tyrosine residues, do αTyr93, αTyr190, and αTyr198 make similar kinds of contributions to agonist binding, or do they play different roles? Important studies using conventional site-directed mutagenesis have addressed this issue, most typically with a tyrosine to phenylalanine mutation (12–15). This could be considered to address whether the hydroxyl group of the tyrosine is important. In the current system, the tyrosine to phenylalanine mutation leads to increases in the ACh EC_{50} by factors of 8.8, 12, and 4.5 for α93, α190, and α198, respectively (Table 1). Others have seen the same trend, although the exact EC_{50} ratios are different (13, 15). Qualitatively, it appears that the hydroxyl group is important at all three sites. Detailed analyses of the conventional mutants, including studies with competitive antagonists, have led others to propose that α93 and α198 are in qualitatively different environments (15). Although one could debate the extent to which general conclusions can be reached based on a single type of structural change, the unnatural amino acid methodology provides decisive data by enabling the evaluation of a range of residues, including both more subtle and more substantial variations on the aromatic theme.

The unnatural amino acid methodology has its broadest application to ligand binding studies if it is also combined with variations in ligand structure. We have therefore performed comparative experiments with three related but structurally distinct agonists, i.e., nicotine, TMA, and ACh.

TABLE 1

ACh EC_{50} values for mutations near the agonist binding site

The residues are listed in the order of Fig. 1.

	EC_{50}		
	α93	α190	α198
		μM	
3-F-Tyr	38	NR[a]	140
F_4-Tyr	44	NR	130
2-F-Tyr	44	NR	350
Tyr (wild-type)	49	49	49
4-COOH-Phe	150	—[b]	670
4-Me-Phe[c]	360	—	160
4-NH_2-Phe	360	900	280
4-MeO-Phe	390	700	84
Phe	430	570	220
Homo-Tyr	460	—	260
DOPA	460	620	730
3-OH-Phe	470	920	770
4-Ac-Phe	570	—	330
4-F-Phe	—	NR	140
3-MeO-Phe	—	—	670
4-Cl-Phe	—	—	95

[a] NR, no response from efforts to incorporate the unnatural residue.
[b] —, the experiment was not attempted.
[c] Me, methyl; MeO, methoxy; Ac, acetyl.

Experimental Procedures

Materials. *Fok*I restriction endonuclease and T4 RNA ligase were purchased from New England Biolabs (Beverly, MA). T7 RNA polymerase was purified, using the method of Grodberg and Dunn (16), from the overproducing *Escherichia coli* strain BL21 harboring the plasmid pAR1219 (17). THF was distilled from sodium benzophenone ketyl. Methylene chloride and acetonitrile were distilled from CaH_2. Reported synthetic yields refer to material dried to constant weight under vacuum (typically 50 mtorr). Flash chromatography was on 230–400-mesh silica gel with the solvent indicated. All NMR shifts are reported as δ ppm downfield from trimethylsilane. ^1H NMR spectra were recorded at 300 MHz in $CDCl_3$ and ^{13}C NMR spectra at 75 MHz in $CDCl_3$ using a GE QE-300 spectrometer, except where noted. FAB, DCI, ESI, and HRMS determinations were performed at the University of California, Riverside (Riverside, CA). Melting points were obtained on a Thomas-Hoover apparatus and are uncorrected. All reagents were obtained from Aldrich Chemical Co. (Milwaukee, WI), Sigma Chemical Co. (St. Louis, MO), or other commercial sources where not explicitly noted. Amino acids and derivatives are of the L-configuration unless otherwise noted.

tRNA gene construction and synthesis. The genes for our original modified yeast $tRNA^{Phe}$ CUA (*MN3*) (1) and *Tetrahymena thermophila* $tRNA^{Gln}$ CUA having a guanine at position 73 (*THG73*) (18) were constructed from eight overlapping synthetic DNA oligonucleotides and cloned into pUC19, giving the plasmids pMN3 and pTHG73, respectively. The genes each contained an upstream T7 RNA polymerase promoter and a downstream *Fok*I restriction site. Template DNA for transcription of tRNA lacking the 3′-terminal C75 and A76 was prepared by digesting the plasmid DNA with *Fok*I restriction endonuclease. *In vitro* transcription of the linearized DNA template and purification of the truncated MN3 and THG73 RNA products were performed as described previously (19).

Mutagenesis and mRNA synthesis. Mouse muscle α, β, γ, and δ nAChR subunits containing the TAG codon and/or 9′-leucine to serine mutants were generated using the Clontech Transformer kit (Clontech, Palo Alto, CA). mRNAs for the wild-type and mutant subunits were prepared by *in vitro* transcription of the appropriate linearized plasmid construct using the Ambion Magic Message machine kit (Ambion, Austin, TX). As before (1), the stop codon in the δ subunit was mutated from TAG to TGA to avoid complications.

Oocyte microinjections and electrophysiological measurements. Before microinjection, the ligated NVOC-aminoacyl-tRNA was renatured by heating to 65° for 3 min in 1 mM sodium acetate, pH 4.5. The NVOC protecting group was subsequently removed by irradiating the sample for 5 min with a 600-W xenon lamp equipped with WG-335 and UG-11 filters (Schott, Duryea, PA). *X. laevis* oocytes were microinjected (50 nl) with either nAChR α93UAG:β:γ:δ mRNA at a concentration ratio of 4:1:1:1 or 100:1:1:1 (12.5–25 ng of total mRNA) or nAChR α198UAG:β:γ:δ mRNA at a concentration ratio of 100:1:1:1 (16 ng of total mRNA) and the desired acylated tRNA (1–25 ng), using published methods (20).

Electrophysiological measurements were carried out 18–30 hr after injection, using a two-electrode voltage-clamp circuit. Oocytes were bathed in solutions containing 5 mM HEPES-NaOH, pH 7.4, 96 mM NaCl, 2 mM KCl, 1 mM $MgCl_2$, and 1 μM atropine. Macroscopic ACh-, nicotine-, or TMA-induced currents were recorded in response to bath application of the desired agonist concentration, at a holding potential of −80 mV. All numerical and plotted data are from mea-

surements obtained for four to eight individual oocytes and are reported as the mean ± standard error. Individual dose-response relations were fit to the Hill equation, $I/I_{max} = 1/[1 + (EC_{50}/[A])^{n_H}]$, where I is the current for agonist concentration $[A]$, I_{max} is the maximal current, EC_{50} is the concentration to elicit a half-maximal response, and n_H is the Hill coefficient.

Ligation of dCA-amino acids to suppressor tRNAs. The NVOC-protected dCA-amino acids were coupled to the MN3 or THG73 *Fok*I runoff transcripts using T4 RNA ligase (21). Ligation reaction mixtures contained 42 mM HEPES-KOH, pH 7.4, 10% (v/v) DMSO, 4 mM dithiothreitol, 20 mM $MgCl_2$, 0.2 mg/ml bovine serum albumin, 150 μM ATP, 10 μM tRNA transcript, 300 μM NVOC-protected dCA-amino acid, and 2000 units/ml T4 RNA ligase. After incubation at 37° for 2 hr, the reaction mixtures were extracted once with an equal volume of phenol/$CHCl_3$/isoamyl alcohol (25:24:1, pH 4.5) and once with an equal volume of $CHCl_3$/isoamyl alcohol (24:1, pH 4.5), precipitated with 2.5 volumes of ethanol at −20°, dried, resuspended in 1 mM sodium acetate, pH 4.5, and stored at −80°. The percentage of ligated product, as judged by electrophoresis on high-resolution, denaturing, 8% polyacrylamide gels, was approximately 90% for MN3 transcripts and only 30% for THG73 transcripts. The reported quantities of all ligated tRNAs have been corrected for ligation efficiency.

General procedure for synthesis of aminoacyl-dCA: dCA-NVOC-4-nitroveratrylcarboxyphenylalanine. The dinucleotide dCA was prepared as reported previously (22), with a few modifications, as follows: 1) the dinucleotide coupling, oxidation, and deprotection with *p*-toluenesulfonic acid were performed in one vessel; 2) the desalting of dCA was accomplished by redissolving the compound in filtered water (Millipore, Bedford, MA), freezing the solution, and lyophilizing it to obtain a fluffy material; and 3) the tetra-*n*-butylammonium salt of the dinucleotide was formed by mixing the proper amount of tetra-*n*-butylammonium hydroxide (1 M in MeOH) with a solution of dCA in water. Freezing and lyophilization provided a white fluffy solid. The solid was stored at −80°, and it was fully reactive after 1 year of storage. To a solution of 18.0 mg of dCA (tetrabutylammonium salt, ~15 mmol) in 400 μl of anhydrous DMF under argon was added 51 mg of NVOC-4-(nitroveratrylcarboxy)phenylalanine cyanomethyl ester (75 mmol, 5 equivalents; see below). The clear pale yellow solution was stirred for 3 hr and then quenched with 200 μl of 25 mM ammonium acetate, pH 4.5. In many cases, shorter reaction times and only 2–3-fold excess cyanomethyl ester was sufficient. In some cases, however, reaction was incomplete, as monitored by analytical high performance liquid chromatography; a spatula tip of tetrabutylammonium acetate forced the reaction to completion. The crude product was purified by reverse-phase, semi-preparative, high performance liquid chromatography (Whatman Partisil 10 ODS-3 column, 9.4 mm × 50 cm), using a gradient from 25 mM ammonium acetate, pH 4.5, to CH_3CN. The appropriate fractions were combined, frozen, and lyophilized. To remove ammonium ions, which inhibit T4 RNA ligase in the ligation of the product to the tRNA, the white solid was redissolved in 10 mM acetic acid/CH_3CN, frozen, and lyophilized, providing 14 mg (75%) of the desired product as a fluffy white solid. Small amounts of material were quantified by their UV-visible spectra, assuming $\epsilon_{350} \sim 6350$/nitroveratryl group. To avoid promoting deaminoacylation, solutions of the product were always kept acidic (pH ≤ 4.5).

Nitroveratryl chloride. To a solution of 4.26 g of nitroveratryl alcohol (20.0 mmol; Lancaster, Windham, NH) in 150 ml of dry CH_2Cl_2 under argon (a small amount of material remained undissolved) was added 1.9 ml of thionyl chloride (26.0 mmol, 1.3 equivalents). The solution was stirred in the dark for 3 hr, after which time it turned dark brown, and was rotary-evaporated to a solid, which was filtered through silica with CH_2Cl_2. The filtrate was rotary-evaporated, providing 4.07 g (88%) of a light yellow solid [^{1}H NMR ($CDCl_3$): δ 7.69 (s, 1 H), 7.11 (s, 1 H), 5.01 (s, 2 H), 4.02 (s, 3 H), 3.97 (s, 3 H); ^{13}C NMR ($CDCl_3$): δ 153.38, 148.71, 140.25, 127.24, 112.80, 108.37, 56.61, 56.53, 43.67].

NVOC-Cl. To a mixture of 4.00 g of nitroveratryl alcohol (18.76 mmol) in 200 ml of dry CH_2Cl_2 under argon, cooled in an ice-water bath, was added 1.6 ml of pyridine (19.78 mmol, 1.05 equivalents). To the resulting pale yellow solution was added, in one portion, 2.78 g of triphosgene (9.37 mmol, 1.5 equivalents of phosgene). After 10 min, the solution was rotary-evaporated to a pale brown solid and partially redissolved in 50 ml of CH_2Cl_2. The mixture was filtered through silica, using more CH_2Cl_2 to dissolve the remaining material. The filtrate was rotary-evaporated and dried to provide 4.77 g of crude material. This was recrystallized from toluene (55° to −20°), providing 3.802 g (74%) of NVOC-Cl as light orange crystals [^{1}H NMR ($CDCl_3$): δ 7.76 (s, 1 H), 7.02 (s, 1 H), 5.73 (s, 2 H), 4.03 (s, 3 H), 3.99 (s, 3 H); ^{13}C NMR ($CDCl_3$): δ 153.65, 150.27, 148.84, 139.78, 124.11, 110.38, 108.28, 69.79, 56.48, 56.42].

NVOC-tyrosine *t*-butyl ester. To a mixture of 870 mg of L-tyrosine *t*-butyl ester (3.67 mmol) and 583 mg of Na_2CO_3 (5.50 mmol, 1.5 equivalents) in 20 ml each of water and THF (two clear layers) was added a solution of 1.003 g of NVOC-Cl (3.64 mmol, 1.0 equivalent) in 25 ml of THF. After 15 min the cloudy yellow mixture was rotary-evaporated and partitioned between 10 ml of water and 30 ml of CH_2Cl_2. The layers were separated and the aqueous layer was extracted with 3 × 10 ml of CH_2Cl_2. The organic layers were combined, dried (over Na_2SO_4), and filtered. The crude material was chromatographed (CH_2Cl_2 to 5:1 CH_2Cl_2/ethyl acetate), affording 1.735 g (100%) of a pale yellow foamy solid [^{1}H NMR ($CDCl_3$): δ 7.68 (s, 1 H), 6.99 (d, J = 8.4 Hz, 1 H), 6.97 (s, 1 H), 6.70 (d, J = 8.4 Hz, 1 H), 6.65 (s, 1 H), 5.56 (d, J = 8.3 Hz, 1 H), 5.54 and 5.45 (AB, J = 15.2 Hz, 1 H), 4.50 (dt, J = 8.3 and 6.1 Hz, 1 H), 3.92 (s, 3 H), 3.91 (s, 3 H), 3.05 (dd, J = 14.2 and 5.9 Hz, 1 H), 2.97 (dd, J = 14.2 and 6.5 Hz, 1 H), 1.44 (s, 9 H); ^{13}C NMR ($CDCl_3$): δ 170.97, 155.43, 155.12, 153.54, 147.80, 139.27, 130.29, 128.08, 127.12, 115.25, 109.52, 107.95, 82.55, 63.72, 56.28, 56.21, 55.30, 37.12, 27.84; FAB-MS: MH^+ *m/z* 477 (13%), 421 (16%), 377 (32%), 196 (100%); HRMS: calculated for $C_{23}H_{29}N_2O_9$, 477.1873; found, 477.1878].

NVOC-4-(trifluoromethanesulfonyl)phenylalanine *t*-butyl ester. A solution of 1.735 g of NVOC-tyrosine *t*-butyl ester (3.64 mmol) and 1.00 ml of triethylamine (7.17 mmol, 2.0 equivalents) in 25 ml of dry CH_2Cl_2 was cooled to −78° (dry ice/acetone bath) under argon. Triflic anhydride (0.75 ml, 4.45 mmol, 1.23 equivalents) was added over about 20 sec. After 10 min the clear yellow solution was quenched at −78° with 10 ml of water and was allowed to warm to room temperature. The layers were gently shaken and separated, and the aqueous layer was extracted with 2 × 10 ml of CH_2Cl_2. The organic layers were combined, dried (over Na_2SO_4), and filtered. The crude product was chromatographed (CH_2Cl_2 to 2% ethyl acetate/CH_2Cl_2), providing 2.027 g (91%) of a pale yellow foamy solid [^{1}H NMR ($CDCl_3$): δ 7.70 (s, 1 H), 7.30 (d, J = 8.7 Hz, 2 H), 7.21 (d, J = 8.7 Hz, 2 H), 6.99 (s, 1 H), 5.55 (d, J = 8.3 Hz, 1 H), 5.51 (m, 2 H), 4.55 (m, 1 H), 3.97 (s, 3 H), 3.95 (s, 3 H), 3.14 (d, J = 6.3 Hz, 2 H), 1.39 (s, 9 H); ^{13}C NMR ($CDCl_3$): δ 170.11, 155.05, 153.48, 148.45, 148.01, 139.56, 136.85, 131.12, 127.70, 121.18, 109.85, 108.01, 118.60 (quartet for CF_3, $^1J_{C-F}$ = 321 Hz), 82.82, 63.76, 56.32, 56.25, 54.98, 37.63, 27.75; DCI-MS: MNH_4^+ *m/z* 626 (43%), 370 (100%); HRMS: calculated for $C_{24}H_{31}N_3O_{11}F_3S$, 626.1631; found, 626.1665].

NVOC-4-carboxyphenylalanine *t*-butyl ester. A mixture of 1.00 g of NVOC-4-(trifluoromethanesulfonyl)phenylalanine *t*-butyl ester (1.64 mmol), 1.29 g of potassium acetate (13.1 mmol, 8 equivalents), and 365 mg of 1,1′-bis(diphenylphosphino)ferrocene (0.658 mmol, 0.40 equivalent) in 15 ml of anhydrous DMSO was degassed with four vacuum/argon cycles. To the mixture was added 38 mg of palladium acetate (0.169 mmol, 0.10 equivalent), and carbon monoxide was bubbled through for 5 min. The mixture was kept under CO with a CO-filled balloon and was heated to 85° (water bath). After 30 min, the mixture was cooled and quenched with 25 ml each of ethyl acetate and 3 NHCl. The layers were separated, and the aqueous phase was extracted with 15 ml of ethyl acetate. The organic layers were combined, dried (over Na_2SO_4), and filtered, and the material was chromatographed (CH_2Cl_2 to ethyl acetate to 5% acetic

acid/ethyl acetate), giving 384 mg (46%) of the desired product [^{1}H NMR ($CDCl_3$): δ 10.29 (br s, 1 H), 8.00 (d, J = 8.0 Hz, 2 H), 7.70 (s, 1 H), 7.30 (d, J = 8.0 Hz, 2 H), 7.00 (s, 1 H), 5.83 (d, J = 8.3 Hz, 1 H), 5.56 and 5.48 (AB, J = 15.2 Hz, 4 H), 4.66 (m, 1 H), 3.94 (s, 3 H), 3.93 (s, 3 H), 3.19 (m, 2 H), 1.44 (s, 9 H); ^{13}C NMR ($CDCl_3$): δ 170.92, 170.65, 155.25, 153.53, 147.91, 142.18, 139.41, 130.15, 129.48, 128.24, 127.96, 109.66, 108.00, 82.95, 63.71, 56.27, 56.24, 54.93, 38.19, 27.83; FAB-MS: MNa^+ m/z 527 (<1%), MH^+ 505 (5%), $(M-H)^{+\cdot}$ 503 (7%), 314 (47%), 268 (65%), 210 (48%), 196 (100%), 164 (68%); HRMS: calculated for $C_{24}H_{28}N_2O_{10}Na$, 527.1642; found, 527.1653].

NVOC-4-(nitroveratrylcarboxy)phenylalanine *t*-butyl ester. A mixture of 161 mg of NVOC-4-carboxyphenylalanine *t*-butyl ester (0.319 mmol), 88 mg of nitroveratryl alcohol (0.413 mmol, 1.3 equivalents), 74 mg of dicyclohexylcarbodiimide (0.359 mmol, 1.13 equivalents), 9 mg of dimethylaminopyridine (0.074 mmol, 0.23 equivalent), and 10 ml of CH_2Cl_2 was stirred for 2 hr under argon and then filtered through Celite. The filtrate was rotary-evaporated and chromatographed (CH_2Cl_2 to 9:1 CH_2Cl_2/ethyl acetate), providing 129 mg (58%) of a pale yellow solid [^{1}H NMR ($CDCl_3$): δ 8.02 (d, J = 8.1 Hz, 2 H), 7.74 (s, 1 H), 7.69 (s, 1 H), 7.31 (d, J = 8.1 Hz, 2 H), 7.10 (s, 1 H), 6.97 (s, 1 H), 5.75 (s, 2 H), 5.55 (d, J = 7.9 Hz, 1 H), 5.52 and 5.46 (AB, J = 14.9 Hz, 1 H), 4.60 (m, 1 H), 3.97 and 3.95 (each s, total 12 H), 3.19 (m, 2 H), 1.42 (s, 9 H); ^{13}C NMR ($CDCl_3$): δ 170.12, 165.55, 155.06, 153.45, 153.34, 148.15, 147.92, 142.04, 139.91, 139.44, 129.62, 129.57, 128.30, 127.78, 126.91, 110.37, 109.71, 108.12, 107.96, 82.69, 63.67, 63.51, 56.27, 56.23, 54.86, 38.12, 27.80; FAB-MS: MH^+ m/z 700 (2%), $M^{+\cdot}$ 699 (2%), 268 (21%), 196 (100%); HRMS: calculated for $C_{33}H_{38}N_3O_{14}$, 700.2354; found, 700.2373].

NVOC-4-(nitroveratrylcarboxy)phenylalanine cyanomethyl ester. To a solution of 129 mg of NVOC-4-(nitroveratrylcarboxy)phenylalanine *t*-butyl ester (0.184 mmol) and 81 mg of 1,4-dimethoxybenzene (0.586 mmol, 3.2 equivalents, as a cation scavenger) in 2 ml of dry CH_2Cl_2 under argon was added 2 ml of TFA. After 2 hr, the volatile compounds were removed under vacuum, and the resulting yellow-green solid was used directly in the next step. To this solid under argon was added 1 ml each of dry DMF and chloroacetonitrile (15.8 mmol, 86 equivalents) and then 80 μl of triethylamine (0.57 mmol, 3.0 equivalents). After 4 hr, the volatile compounds were removed under vacuum, leaving a filmy solid, which was chromatographed (CH_2Cl_2 to 5:1 CH_2Cl_2/ethyl acetate), affording 100 mg (79% for two steps) of an off-white solid [^{1}H NMR ($CDCl_3$): δ 8.06 (d, J = 8.2 Hz, 2 H), 7.75 (s, 1 H), 7.71 (s, 1 H), 7.28 (d, J = 8.2 Hz, 2 H), 7.10 (s, 1 H), 6.93 (s, 1 H), 5.76 (s, 2 H), 5.56 and 5.46 (AB, J = 14.5 Hz, 1 H), 5.28 (d, J = 8.0 Hz, 1 H), 4.84 and 4.70 (AB, J = 15.6 Hz, 1 H), 4.68 (m, 1 H), 3.97 (s) and 3.96 (m) (total 12 H), 3.28 and 3.20 (AB, J = ~10 and 6.5 Hz, 10 H); DCI-MS: MNH_4^+ m/z 700 (13%), 231 (100%); HRMS: calculated for $C_{31}H_{34}N_5O_{14}$, 700.2102; found, 700.2067; FAB-MS: MNa^+ m/z 705 (<1%), MH^+ 683 (61%); HRMS: calculated for $C_{31}H_{30}N_4O_{14}Na$, 705.1656; found, 705.16654].

dCA-NVOC-4-nitroveratrylcarboxyphenylalanine. This compound was prepared by the ligation procedure described above [ESI-MS: $(M+Cl)^-$ m/z 1296 (10%), M^- 1261 (24%), $(M-H)^{2-}$ 630 (100%); calculated for $C_{48}H_{53}N_{11}O_{26}P_2$, 1261].

L-*m*-Tyrosine. A solution of 905 mg of DL-*m*-tyrosine methyl ester (3.91 mmol) in 15 ml of water at 37° (water bath) was adjusted to pH ~5.0 with ~1 ml of 0.5 M LiOH. A solution of 100 mg of α-chymotrypsin (Sigma no. C4129, type II, 5000 units) was dissolved in water (23). The enzyme and more LiOH were added dropwise in alternation over several minutes until all of the enzyme was added; the pH was maintained near 5.0 as indicated by a pH meter. After several additional minutes, the pH was falling only very slowly and was maintained near 5.0 with a drop of LiOH solution every few minutes. Within 3 hr, a significant amount of cloudy white material was apparent. After 8 hr, ~7.5 ml of 0.5 M LiOH (~3.8 mmol) had been added, and the mixture was filtered through Celite, rinsing with water. The clear colorless filtrate was frozen and lyophilized, providing an off-white solid. This was swirled with 25 ml of absolute ethanol for ~1 min and then filtered (through a fritted funnel), yielding a white solid that was rinsed well with ethanol and dried [383 mg (107% of the theoretical amount of the L-enantiomer; m.p. (open capillary), browns near 225°, melts at 257.5–259.0° (dec); literature m.p. (33), 256–260°]. The material was of suitable purity for the next step.

***m*-Tyrosine methyl ester.** Through a mixture of 383 mg of L-*m*-tyrosine (nominally 2.11 mmol) and 20 ml of anhydrous MeOH in a 250-ml round-bottomed flask, cooled in ice water, was bubbled gaseous HCl. After 15 min, the pale yellow solution with a small amount of undissolved solid was refluxed under a $CaCl_2$ drying tube. After 2 hr, half of the solvent was distilled off, and the remaining mixture was rotary-evaporated to a pale yellow oil. This was dried under vacuum to provide a pale yellow foamy solid, which nearly completely redissolved in 3 ml of MeOH. To the solution was added 15 ml of ether, immediately precipitating a pale yellow amorphous solid. The mixture was rotary-evaporated, and the resulting solid was used directly in the next step.

NVOC-*m*-tyrosine methyl ester. The material from the previous step was mixed with 447 mg of Na_2CO_3 (4.22 mmol), 15 ml of water, and 5 ml of dioxane. The slightly cloudy mixture was stirred as a solution of 582 mg of NVOC-Cl (2.11 mmol) in 15 ml of dioxane was added dropwise over 15 min. After 30 min, the cloudy mixture was rotary-evaporated to ~1/3 volume and quenched with 4.5 ml of 1 NHCl, yielding a very cloudy mixture. This was extracted gently with 25 ml of CH_2Cl_2 and then vigorously with 2 × 10 ml of CH_2Cl_2. The organic layers were combined, dried (over $MgSO_4$), and filtered. The crude material was chromatographed (CH_2Cl_2 to 3:1 CH_2Cl_2/ethyl acetate), providing 444 mg of a sticky, slightly foamy, pale yellow solid (48% for two steps from L-*m*-tyrosine) [^{1}H NMR ($CDCl_3$): δ 7.66 (s, 1 H), 7.11 (t, J = 8.0 Hz, 1 H), 6.93 (s, 1 H), 6.79 (br s, 1 H), 6.69 (d, J = 8.2 Hz, 1 H), 6.64 (m, 2 H), 5.65 (d, J = 8.3 Hz, 1 H), 5.47 (s, 2 H), 4.64 (m, 1 H), 3.92 (s, 3 H), 3.91 (s, 3 H), 3.73 (s, 3 H), 3.12 (dd, J = 14.0 and 5.2 Hz, 1 H), 3.00 (dd, J = 14.0 and 6.9 Hz, 1 H); ^{13}C NMR ($CDCl_3$): δ 172.04, 156.27, 155.44, 153.56, 147.89, 139.27, 137.09, 129.66, 127.84, 120.79, 116.00, 114.15, 109.71, 107.98, 63.90, 56.35, 56.22, 54.67, 52.40, 37.50; FAB-MS: MH^+ m/z 435 (17%), $M^{+\cdot}$ 434 (10%), 391 (30%), 196 (100%); HRMS: calculated for $C_{20}H_{23}N_2O_9$, 435.1404; found, 435.1403].

NVOC-3-methoxyphenylalanine methyl ester. A mixture of 444 mg of NVOC-*m*-tyrosine methyl ester (1.02 mmol), 282 mg of K_2CO_3 (2.04 mmol, 2.0 equivalents), 320 μl of methyl iodide (5.1 mmol, 5 equivalents), and 10 ml of dry acetonitrile was refluxed for 3 hr under argon and then rotary-evaporated to a yellow solid. This was filtered through silica (9:1 CH_2Cl_2/ethyl acetate), yielding 441 mg (96%) of a pale yellow filmy solid [^{1}H NMR ($CDCl_3$): δ 7.69 (s, 1 H), 7.20 (t, J = 7.9 Hz, 1 H), 6.95 (s, 1 H), 6.78 (dd, J = 8.2 and 2.3 Hz, 1 H), 6.71 (d, J = 7.6 Hz, 1 H), 6.68 (d, J = 1.8 Hz, 1 H), 5.51 (m, 3 H), 4.67 (m, 1 H), 3.94 (s, 3 H), 3.93 (s, 3 H), 3.76 (s, 3 H), 3.75 (s, 3 H), 3.15 (dd, J = 14.0 and 5.4 Hz, 1 H), 3.06 (dd, J = 14.0 and 6.6 Hz, 1 H); ^{13}C NMR ($CDCl_3$): δ 171.87, 159.58, 155.14, 153.54, 147.81, 139.25, 137.05, 129.50, 128.14, 121.27, 114.86, 112.20, 109.32, 107.91, 63.58, 56.28, 56.21, 54.96, 54.61, 52.29, 37.76; FAB-MS: MH^+ m/z 449 (9%), $M^{+\cdot}$ 448 (7%), 405 (37%), 196 (100%); HRMS: calculated for $C_{21}H_{24}N_2O_9$, 448.1482; found, 448.1492].

NVOC-3-methoxyphenylalanine. To a solution of 438 mg of NVOC-3-methoxyphenylalanine methyl ester (0.977 mmol) in 10 ml of CH_2Cl_2 were added 10 ml of 1 NNaOH and 10 drops of the phase-transfer catalyst Aliquat 336 (Aldrich, Milwaukee, WI). The mixture was vigorously stirred for 2 hr, and another 10 drops of Aliquat 336 were added. After an additional 3 hr, another 5 ml of 1 NNaOH and 10 drops of Aliquat 336 were added. After an additional 4 hr, the clear layers were separated. The aqueous layer was extracted with 2 × 5 ml of CH_2Cl_2. The organic layers were combined, dried (over $MgSO_4$), and filtered. The crude product was chromatographed (CH_2Cl_2 to ethyl acetate to 1% acetic acid/ethyl acetate), affording 362 mg (85%) of a pale yellow foamy solid [^{1}H NMR

($CDCl_3$): δ 9.27 (s, 1 H), 7.68 (s, 1 H), 7.20 (t, J = 7.8 Hz, 1 H), 6.93 (s, 1 H), 6.76 (m, 3 H), 5.63 (d, J = 8.3 Hz, 1 H), 5.50 (m, 2 H), 4.69 (m, 1 H), 3.93 (s, 3 H), 3.88 (s, 3 H), 3.75 (s, 3 H), 3.22 (dd, J = 14.0 and 7.2 Hz, 1 H), 3.06 (dd, J = 14.0 and 5.0 Hz, 1 H); ^{13}C NMR ($CDCl_3$): δ 175.80, 159.52, 155.49, 153.50, 147.82, 139.24, 137.00, 129.57, 127.88, 121.38, 114.94, 112.24, 109.44, 107.91, 63.79, 56.21, 56.19, 54.98, 54.50, 37.34; FAB-MS: MNa^+ m/z 457 (6%), $M^{+\cdot}$ 434 (10%), 391 (30%), 196 (100%); HRMS: calculated for $C_{20}H_{22}N_2O_9$, 434.1325; found, 434.1324].

NVOC-3-methoxyphenylalanine cyanomethyl ester. To a solution of 362 mg of NVOC-3-methoxyphenylalanine (0.833 mmol) in 2 ml each of dry DMF and chloroacetonitrile (31.6 mmol, 38 equivalents) under argon was added 350 μl of triethylamine (2.51 mmol, 3.0 equivalents). After 2 hr, the volatile compounds were removed under vacuum, leaving a light yellow pasty solid. This was chromatographed (CH_2Cl_2 to 7:1 CH_2Cl_2/ethyl acetate), yielding 378 mg (96%) of a pale yellow foamy solid [^1H NMR ($CDCl_3$): δ 7.67 (s, 1 H), 7.22 (t, J = 7.9 Hz, 1 H), 6.92 (s, 1 H), 6.80 (dd, J = 8.2 and 2.1 Hz, 1 H), 6.74 (d, J = 7.6 Hz, 1 H), 6.70 (d, J = 1.6 Hz, 1 H), 5.59 (d, J = 8.3 Hz, 1 H), 5.52 and 5.43 (AB, J = 15.2 Hz, total 2 H), 4.82 and 4.71 (AB, J = 15.7 Hz, total 2 H), 4.70 (m, 1 H), 3.92 (2 s, 3 H each), 3.77 (s, 3 H), 3.16 (dd, J = 14.0 and 5.7 Hz, 1 H), 3.07 (dd, J = 14.0 and 7.1 Hz, 1 H); ^{13}C NMR ($CDCl_3$): δ 170.31, 159.68, 155.14, 153.47, 147.85, 139.25, 136.27, 129.76, 127.62, 121.12, 114.73, 113.77, 112.50, 109.49, 107.88, 63.78, 56.25, 56.17, 55.01, 54.44, 48.88, 37.33; FAB-MS: $M^{+\cdot}$ m/z 473 (10%), 430 (27%), 196 (100%); HRMS: calculated for $C_{22}H_{23}N_3O_9$, 473.1434; found, 473.1444].

dCA-NVOC-3-methoxyphenylalanine. This compound was prepared by the ligation procedure described above [ESI-MS: M−H m/z 1051; calculated for $C_{39}H_{46}N_{10}O_{21}P_2$, 1052].

Cu(L-*m*-tyrosine)$_2$. To a mixture of 420 mg of L-m-tyrosine (2.32 mmol) and 273 mg of NaOH (6.9 mmol, 3.0 equivalents) in 2.5 ml of water was added a solution of 275 mg $CuSO_4 \cdot 5H_2O$ (1.10 mmol) in 2 ml of water. The mixture was stirred at 60° (water bath) for 10 min, giving a slightly cloudy, dark olive green mixture. This was cooled to room temperature and acidified with 1 ml of acetic acid, providing a blue mixture with clearly visible precipitate. After standing for 1 hr, the mixture was filtered (through a fritted funnel), giving a purple precipitate and a clear bright green filtrate. The solid was washed with 10 ml of water and 20 ml of acetone and then dried, affording 364 mg (74%) of the desired product, which was used directly in the next step.

***O*-Nitroveratryl-*m*-tyrosine.** To a mixture of 364 mg of Cu(L-m-tyrosine)$_2$ (0.859 mmol) in 12 ml of DMF and 4 ml of water was added 328 mg of K_2CO_3 (1.72 mmol, 1.0 equivalent/tyrosine ring). After several minutes, to the dark blue opaque mixture was added 438 mg of nitroveratryl chloride (1.89 mmol, 1.1 equivalent/tyrosine ring). After 24 hr, the dark green-brown mixture was filtered (in a fritted funnel), retaining a light blue solid and yielding a dark green-brown filtrate. The solid was washed with 10 ml each of 75% aqueous DMF, water, and acetone and then dried, affording crude Cu[L-m-tyrosine(O-nitroveratryl)$_2$]$_2$ as a brittle dark blue solid. This was stirred with 5 ml of 1 NHCl for 1 hr, after which time the very pale yellow cloudy mixture was filtered (in a fritted funnel). The retained off-white pasty solid was washed with 10 ml each of 1 NHCl, water, and acetone and then dried to provide 136 mg (42% overall) of the desired material [^1H NMR (DMSO-d_6): δ 7.72 (s, 1 H), 7.32 (s, 1 H), 7.26 (t, J = 7.8 Hz, 1 H), 6.97 (s, 1 H), 6.94 (d, J ~ 8 Hz, 1 H), 6.87 (d, J = 7.6 Hz, 1 H), 5.40 (s, 2 H), 4.06 (m, 1 H), 3.87 (s, 6 H), 3.07 (m, 2 H), plus several small peaks presumably resulting from impurities]. The material was sufficiently pure to continue.

NVOC-*O*-nitroveratryl-*m*-tyrosine. A mixture of 131 mg of O-nitroveratryl-m-tyrosine (0.348 mmol), 74 mg of Na_2CO_3 (0.698 mmol, 2.0 equivalents), 5 ml of water, and 5 ml of dioxane was stirred as a solution of 96 mg of NVOC-Cl (0.348 mmol, 1.0 equivalent) in 3 ml of dioxane was added at once. Within 5 min, a clear yellow solution was formed. After 30 min, 0.8 ml of 1 NHCl and 25 ml of CH_2Cl_2 were added and the layers were separated. The aqueous layer was extracted with 3 × 10 ml of CH_2Cl_2. The organic layers were combined, dried (over Na_2SO_4), and filtered. The crude material was chromatographed (CH_2Cl_2 to ethyl acetate to 0.5% acetic acid/ethyl acetate), providing 168 mg (78%) of a yellow oil, which solidified upon standing [^1H NMR ($CDCl_3$): δ 7.74 (s, 1 H), 7.67 (s, 1 H), 7.31 (s, 1 H), 7.23 (t, J = 7.7 Hz, 1 H), 6.93 (s, 1 H), 6.87 (m, 3 H), 5.48 (m, 5 H), 4.73 (m, 1 H), 3.96 (s, 3 H), 3.95 (s, 3 H), 3.92 (s, 3 H), 3.89 (s, 3 H), 3.24 (dd, J = 14.0 and 5.2 Hz, 1 H), 3.11 (dd, J = 14.0 and 6.8 Hz, 1 H); DCI-MS: MNH_4^+ m/z 633 (3%), 231 (100%), 213 (77%), 182 (79%), 180 (76%); HRMS: calculated for $C_{28}H_{33}N_4O_{13}$, 633.2044; found, 633.2052].

NVOC-*O*-nitroveratryl-*m*-tyrosine cyanomethyl ester. To a solution of 168 mg of NVOC-O-nitroveratryl-m-tyrosine (0.273 mmol) in 2 ml each of dry DMF and chloroacetonitrile (31.6 mmol, 38 equivalents) under argon was added 120 μl of triethylamine (0.861 mmol, 3.0 equivalents). After 3 hr, the volatile compounds were removed under vacuum, leaving a yellow solid. This was chromatographed (CH_2Cl_2 to 9:1 CH_2Cl_2/ethyl acetate), affording 176 mg (99%) of a pale yellow solid [^1H NMR ($CDCl_3$): δ 7.77 (s, 1 H), 7.70 (s, 1 H), 7.35 (s, 1 H), 7.29 (t, J = 7.2 Hz, 1 H), 6.94 (m, 1 H), 6.93 (s, 1 H), 6.82 (m, 2 H), 5.58 and 5.45 (AB, J = 14.9 Hz, total 2 H), 5.46 (s, 2 H), 5.29 (d, J = 8.2 Hz, 1 H), 4.85 and 4.71 (AB, J = 15.7 Hz, 1 H), 4.76 (m, 1 H), 3.98 (s, 3 H), 3.97 (s, 3 H), 3.94 (s, 6 H), 3.17 (t, 5.0 Hz, 1 H); DCI-MS: MNH_4^+ m/z 672 (2%), 231 (88%), 213 (91%), 182 (100%), 180 (84%); HRMS: calculated for $C_{30}H_{34}N_5O_{13}$, 672.2153; found, 672.2176].

dCA-NVOC-*O*-nitroveratryl-*m*-tyrosine. This compound was prepared by the ligation procedure described above [FAB-MS: M−H m/z 1232; calculated for $C_{47}H_{53}N_{11}O_{25}P_2$, 1233].

NVOC-DOPA methyl ester. To a solution of 377 mg of L-DOPA methyl ester hydrochloride (1.52 mmol) in 15 ml of water and 5 ml of dioxane under argon was added 320 mg of Na_2CO_3 (3.02 mmol, 2.0 equivalents). The solution rapidly turned brown, despite precautions to exclude air. A solution of 429 mg of NVOC-Cl (1.52 mmol, 1.0 equivalent) in 15 ml of dioxane was added dropwise over 20 min. After an additional 10 min the slightly cloudy mixture was concentrated by rotary-evaporation to provide a cloudier orange-brown mixture. To this was added 3.0 ml of 1 NHCl followed by 20 ml of CH_2Cl_2. The mixture was swirled vigorously and the layers were separated. The aqueous phase was extracted with 3 × 10 ml of CH_2Cl_2. The organic layers were combined, dried (over $MgSO_4$), and filtered. The crude material was chromatographed twice (CH_2Cl_2 to ethyl acetate and then CH_2Cl_2 to 1:1 CH_2Cl_2:ethyl acetate), providing 370 mg (54%) of a yellow foamy solid [^1H NMR ($CDCl_3$): δ 7.62 (s, 1 H), 6.89 (s, 1 H), 6.68 (d, J = 8.0 Hz, 1 H), 6.63 (br s, 3 H), 6.47 (d, J = 8.0 Hz, 1 H), 5.76 (d, J = 8.4 Hz, 1 H), 5.43 (s, 2 H), 4.58 (m, 1 H), 3.89 (s, 3 H), 3.87 (s, 3 H), 3.71 (s, 3 H), 3.03 (dd, J = 14.0 and 5.1 Hz, 1 H), 2.90 (dd, J = 14.0 and 7.0 Hz, 1 H); ^{13}C NMR ($CDCl_3$): δ 172.37, 155.70, 153.59, 147.87, 143.81, 143.06, 139.18, 127.73, 121.14, 115.97, 115.27, 109.66, 107.94, 64.01, 56.29, 56.19, 54.95, 52.47, 37.00; DCI-MS: MNH_4^+ m/z 468 (5%), 212 (100%); HRMS: calculated for $C_{20}H_{26}N_3O_{10}$, 468.1618; found, 468.1591].

NVOC-DOPA(*O*-nitroveratryl)$_2$ methyl ester. A mixture of 361 mg of NVOC-DOPA methyl ester (0.802 mmol), 450 mg of K_2CO_3 (3.26 mmol, 4.1 equivalents), 372 mg of nitroveratryl chloride (1.61 mmol, 2.0 equivalents), and 20 ml of dry acetonitrile was refluxed under argon for 7.5 hr. The very cloudy dark yellow mixture was rotary-evaporated and chromatographed (CH_2Cl_2 to 9:1 CH_2Cl_2/ethyl acetate), affording 436 mg (65%) of a yellow solid [^1H NMR ($CDCl_3$): δ 7.72 (s, 2 H), 7.67 (s, 1 H), 7.38 (2 s, Δδ = 3.0 Hz, each 1 H), 6.96 (s, 1 H), 6.95 (d, J = 8.2 Hz, 1 H), 6.83 (d, J = 1.7 Hz, 1 H), 6.76 (dd, J = 8.2 and 1.7 Hz, 1 H), 5.48 (m, 7 H), 4.65 (m, 1 H), 3.96, 3.95, and 3.93 (each s, total 12 H), 3.83 (s, 6 H), 3.75 (s, 3 H), 3.15 (dd, J = 14.0 and 5.3 Hz, 1 H), 3.06 (dd, J = 14.0 and 6.3 Hz, 1 H); ^{13}C NMR ($CDCl_3$): δ 171.75, 155.11, 153.76, 153.50, 148.41, 147.99, 147.89, 147.54, 139.56, 139.07, 129.87, 128.91, 128.75, 127.73, 122.91, 115.96, 115.29, 109.81, 108.05, 107.92, 68.49, 68.43, 63.71,

56.31, 56.23, 56.15, 54.72, 52.27, 37.37; FAB-MS: MH^+ *m/z* 841; HRMS: calculated for $C_{38}H_{41}N_4O_{18}$, 841.2416; found, 841.2461].

NVOC-DOPA(*O*-nitroveratryl)$_2$. To a solution of 226 mg of NVOC-DOPA(*O*-nitroveratryl)$_2$ methyl ester (0.269 mmol) in 5 ml of CH_2Cl_2 was added 5 ml of 1.01 N NaOH. Three drops of Aliquat 336 were added and the mixture was stirred vigorously. After 15 min, three more drops of Aliquat 336 were added. After a total of 3 hr, six more drops of Aliquat 336 were added. After 1 hr more the layers were separated and the aqueous layer was extracted with 5 ml more of CH_2Cl_2. The organic layers were combined, dried (over $MgSO_4$), and filtered. The crude product was chromatographed (CH_2Cl_2 to ethyl acetate to 1% acetic acid/ethyl acetate), yielding 179 mg (81%) of a pale yellow solid [^{1}H NMR ($CDCl_3$): δ 7.71 (2 s, $\Delta\delta$ = 2.7 Hz, each 1 H), 7.66 (s, 1 H), 7.37 (s, 2 H), 6.95 (m, 2 H), 6.89 (s, 1 H), 6.80 (d, J = 7.9 Hz, 1 H), 5.48 (m, 7 H), 4.68 (m, 1 H), 3.96 (s, 6 H), 3.92 (s, 6 H), 3.82 (s, 6 H), 3.14 (m, 2 H); FAB-MS: MNa^+ *m/z* 849; HRMS: calculated for $C_{37}H_{38}N_4O_{18}Na$, 849.2079; found, 849.2098].

NVOC-DOPA(*O*-nitroveratryl)$_2$ cyanomethyl ester. To a solution of 174 mg of NVOC-DOPA(*O*-nitroveratryl)$_2$ (0.210 mmol) in 1 ml each of dry DMF and chloroacetonitrile (31.6 mmol, 38 equivalents) under argon was added 88 μl of triethylamine (0.63 mmol, 3.0 equivalents). After 2.5 hr, the volatile compounds were removed under vacuum, leaving a yellow solid. This was chromatographed (CH_2Cl_2 to 7:1 CH_2Cl_2/ethyl acetate), providing 174 mg (96%) of a pale yellow solid [^{1}H NMR ($CDCl_3$): δ 7.72 (s, 1 H), 7.71 (s, 1 H), 7.69 (s, 1 H), 7.37 (s, 1 H), 7.36 (s, 1 H), 6.96 (d, J = 8.1 Hz, 1 H), 6.95 (s, 1 H), 6.84 (d, J = 1.6 Hz, 1 H), 6.78 (dd, J = 8.1 and 1.6 Hz, 1 H), 5.57 and 5.43 (AB, J = 14.7 Hz, total 2 H), 5.50 (m, 4 H), 5.30 (d, J = 8.3 Hz, 1 H), 4.85 and 4.69 (AB, J = 15.6 Hz, total 2 H), 4.70 (m, 1 H), 3.97 (s, 3 H), 3.96 (s, 6 H), 3.94 (s, 3 H), 3.84 (s, 3 H), 3.81 (s, 3 H), 3.13 (m, 2 H); FAB-MS: MH^+ *m/z* 866; HRMS: calculated for $C_{39}H_{40}N_5O_{18}$, 866.2368; found, 866.2405].

dCA-NVOC-DOPA(*O*-nitroveratryl)$_2$. This compound was prepared by the ligation procedure described above [ESI-MS: M−H *m/z* 1443; calculated for $C_{56}H_{62}N_{12}O_{30}P_2$, 1444].

NVOC-4-acetylphenylalanine *t*-butyl ester. To an oven-dried, three-necked flask were added 280 mg of NVOC-4-(trifluoromethanesulfonyl)phenylalanine *t*-butyl ester (0.46 mmol), 2.6 mg of palladium acetate (0.025 equivalent), 5.3 mg of 1,3-bis(diphenylphosphino)propane (0.0275 equivalent), and 5 ml of anhydrous DMF (24). To the stirring mixture were added 0.1 ml of diisopropylethylamine (0.57 mmol, 1.25 equivalents) and 0.3 ml of vinyl butyl ether (2.32 mmol, 5 equivalents). The reaction mixture was kept in a 80° sand bath. More reagents were added 6 hr later, i.e., 5 mg of palladium acetate, 10 mg of 1,3-bis(diphenylphosphino)propane, 0.1 ml of diisopropylethylamine, and 0.3 ml of vinyl butyl ether. After stirring overnight, another addition of the aforementioned reagents was made. The reaction was then cooled and quenched by the addition of 10 ml of 3 N HCl. Thirty minutes later, the mixture was extracted with 2 × 20 ml of ethyl acetate, and the organic layer was dried over Na_2SO_4. Column chromatography using ethyl acetate/petroleum ether (30:70) provided 130 mg (56%) of product [^{1}H NMR ($CDCl_3$): δ 7.88 (d, J = 8.5 Hz, 2 H), 7.68 (s, 1 H), 7.28 (d, J = 8.5 Hz, 2 H), 6.95 (s, 1 H), 5.62 (d, J = 7.7 Hz, 1 H), 5.48 (dd, 2 H), 4.58 (m, 1 H), 3.95 (s, 3 H), 3.93 (s, 3 H), 2.58 (s, 3 H), 1.42 (s, 9 H); ^{13}C NMR ($CDCl_3$): δ 198.09, 170.84, 155.76, 154.15, 148.63, 142.40, 136.49, 130.16, 128.98, 128.51, 110.47, 108.70, 83.27, 64.26, 60.85, 56.89, 55.56, 38.70, 28.47, 27.03, 14.70].

NVOC-4-acetylphenylalanine cyanomethyl ester. To a solution of 130 mg (0.258 mmol) of NVOC-4-acetylphenylalanine *t*-butyl ester in 2.5 ml of CH_2Cl_2 was added 2.5 ml of TFA. The mixture was stirred at room temperature for 2 hr. TFA was purged by passing argon through the solution, and the resulting residue was redissolved in 25 ml of CH_2Cl_2, washed with 2 × 25 ml of KH_2PO_4 (1 M), and dried over Na_2SO_4. The solvent was rotary-evaporated. The crude product was dissolved in 0.5 ml of DMF, and then 0.1 ml of chloroacetonitrile (1.58 mmol, 6 equivalents) and 0.1 ml of diisopropylethylamine (0.575 mmol, 2.9 equivalents) were added. The reaction mixture was kept in the dark overnight, diluted with 25 ml of CH_2Cl_2, washed with 2 × 25 ml of KH_2PO_4 (1 M), and dried over Na_2SO_4. Flash column chromatography using ethyl acetate/petroleum ether (50:50) provided 110 mg (88%) of off-white solid [^{1}H NMR ($CDCl_3$): δ 7.86 (d, J = 7.5 Hz, 2 H), 7.63 (s, 1 H), 7.26 (d, J = 7.5 Hz, 2 H), 6.90 (s, 1 H), 5.98 (d, J = 9.0 Hz, 1 H), 5.42 (dd, 2 H), 4.76 (m, 3 H), 3.88 (s, 3 H), 3.84 (s, 3 H), 3.20 (m, 2 H), 2.55 (s, 3 H)].

dCA-NVOC-4-acetylphenylalanine. This compound was prepared by the ligation procedure described above [FAB-MS: M−H *m/z* 1063; calculated for $C_{40}H_{46}N_{10}O_{21}P_2$, 1064].

(−)-Pseudoephedrine-4-methylphenylalaninamide. To a flame-dried Schlenck flask was added 560 mg of LiCl (13.1 mmol, 6 equivalents). The apparatus was flame-dried again. Six milliliters of THF were added, followed by addition of 0.62 ml of diisopropylamine (4.38 mmol, 2 equivalents). At −80°, 2.51 ml of *n*-butyl lithium (1.695 M in hexane, 5.65 mmol, 1.95 equivalents) was added slowly along the inner surface of the flask. The mixture was stirred for 20 min and then a solution of 486 mg of (−)-pseudoephedrine glycinamide (2.19 mmol) in 3 ml of THF was added slowly (25). A yellow opaque mixture resulted, which was further stirred at −80° for 20 min and then at 0° for 20 min, producing a bright yellow slurry. At 0°, a solution of 450 mg of 4-methylbenzylbromide in 2 ml of THF was added, and the yellow color disappeared quickly. The reaction was quenched 2 hr later with 35 ml of HCl (1 N), and the mixture was washed with 35 ml of ethyl acetate. The aqueous layer was basified with approximately 3 ml of 50% NaOH to pH 13–14 and extracted with 4 × 40 ml of CH_2Cl_2, and the organic layer was dried over K_2CO_3. Flash chromatography using triethylamine/MeOH/CH_2Cl_2 (2.5:2.5:95) provided 565 mg (79%) of white solid [^{1}H NMR ($CDCl_3$): δ 7.50–7.10 (m, 9 H), 4.88 (m, 1 H), 4.56 (d, J = 9.4 Hz, 1 H), 3.99 (t, 1 H), 3.44 (m, 3 H), 2.88 (m, 2 H), 2.72 (s, 3 H), 2.43 (s, 3 H), 0.90 (d, J = 6.7 Hz, 3 H); there were also minor rotomer peaks at δ 3.06 (s), 2.46 (s), and 1.09 (d)].

NVOC-4-methylphenylalanine cyanomethyl ester. To a flask containing 550 mg of (−)-pseudoephedrine-4-methylphenylalaninamide (1.69 mmol) were added 5 ml of H_2O and 1.7 ml of 1 N NaOH (1.7 mmol, 1 equivalent). The mixture was refluxed for 3 hr and extracted with 2 × 15 ml of CH_2Cl_2 after cooling to room temperature. The aqueous layer was added in one portion to a stirred solution of 476 mg of NVOC-Cl (1.7 mmol, 1 equivalent) in 10 ml of dioxane. Gas was generated and the mixture was stirred for 25 min, acidified with 1 M KH_2PO_4, and extracted with 2 × 20 ml of CH_2Cl_2. The organic layers were combined and dried over Na_2SO_4. Solvent was then rotary-evaporated and the resulting residue was used directly in the next step. The residue was redissolved in 1 ml of DMF, and 0.4 ml of chloroacetonitrile (6.32 mmol, 3.6 equivalents) and 0.4 ml of diisopropylethylamine (2.3 mmol, 1.36 equivalents) were added. The reaction mixture was kept in the dark overnight, diluted with 40 ml of ethyl acetate, and washed with 2 × 40 ml of KH_2PO_4 (1 M), and the organic layer was dried over Na_2SO_4. Flash chromatography using ethyl acetate/petroleum ether (40:60) provided 430 mg (57% for three steps) of solid [^{1}H NMR ($CDCl_3$): δ 7.71 (s, 1 H), 7.27 (d, J = 9.8 Hz, 2 H), 7.04 (d, J = 9.8 Hz, 2 H), 6.93 (s, 1 H), 5.50 (m, 3 H), 4.80 (m, 3 H), 3.92 (s, 3 H), 3.91 (s, 3 H), 3.13 (m, 2 H), 2.34 (s, 3 H)].

dCA-NVOC-4-methylphenylalanine. This compound was prepared by the ligation procedure described above [FAB-MS: M+H$^+$ *m/z* 1037; calculated for $C_{39}H_{46}N_{10}O_{20}P_2$, 1036].

4-*t*-Butyldimethylsilyloxyphenethyliodide. To a solution of 3.14 g of 4-hydroxyphenethyl alcohol (30 mmol) in 300 ml of dry THF was slowly added 17.75 ml of *n*-butyl lithium (1.695 M in hexane, 30 mmol, 1 equivalent) at −78°. Precipitates formed. The mixture was stirred at −78° for 30 min and then at room temperature for 30 min. The mixture was cooled to −78°, and 4.6 g of *t*-butyldimethylsilyl chloride (30 mmol, 1 equivalent) was added as a solid in one portion. The reaction mixture was slowly warmed to room temperature and kept there for 3 hr. A clear solution resulted. The volatile compounds were removed by rotary-evaporation, and the residue was purified by flash chromatography using ethyl acetate/petroleum ether (10:90),

providing 3.62 g (98% after recovery of starting material) of 4-*t*-butyldimethylsiloxyphenethyl alcohol. This product was then converted to the corresponding mesylate by mixing with 5.4 ml of diisopropylethylamine (88 mmol, 6.1 equivalent) and 1.3 ml of mesyl chloride (16.2 mmol, 1.13 equivalents) in 50 ml of CH_2Cl_2 at 0°. After 40 min, the reaction mixture was washed once with 50 ml of water. CH_2Cl_2 was removed by rotary-evaporation, providing the desired mesylate as a clear oil. The mesylate was then dissolved in 75 ml of acetone, and 23 g of NaI (153 mmol, 10.7 equivalents) was added. The mixture was stirred in the dark overnight. Acetone was removed by rotary-evaporation. The solid was redissolved in water and CH_2Cl_2 (50 ml each; the top layer in this case was CH_2Cl_2). The organic layer was dried over Na_2SO_4. Flash chromatography using petroleum ether provided 4.87 g (91% for three steps) of product as a colorless oil [^{1}H NMR ($CDCl_3$): δ 7.08 (d, 2 H), 6.82 (d, 2 H), 3.78 (t, 2 H), 3.13 (t, 2 H), 1.03 (s, 9 H), 0.24 (s, 6 H); ^{13}C NMR ($CDCl_3$): δ 154.64, 133.62, 129.50, 120.31, 39.87, 25.92, 18.37, 6.63, −4.13].

(−)-Pseudoephedrine-4-*t*-butyldimethylsilyl-homotyrosinamide. To a flame-dried Schlenk flask was added 560 mg of LiCl (13.1 mmol, 6 equivalents). The apparatus was flame-dried again. Six milliliters of THF were added, followed by addition of 0.62 ml of diisopropylamine (4.38 mmol, 2 equivalents). At −80°, 2.51 ml of *n*-butyl lithium (1.695 M in hexane, 5.65 mmol, 1.95 equivalents) was added slowly along the inner surface of the flask. The mixture was stirred for 20 min and then a solution of 486 mg of (−)-pseudoephedrine glycinamide (2.19 mmol) in 3 ml of THF was added slowly. A yellow opaque mixture resulted, which was further stirred at −80° for 20 min and then at 0° for 20 min, which produced a bright yellow slurry. At 0°, a solution of 870 mg of 4-*t*-butyldimethylsiloxyphenethyliodide in 3 ml of THF was added. The reaction mixture was kept at 4° overnight. Forty milliliters of water were added to the reaction mixture, the mixture was extracted with 4 × 40 ml of CH_2Cl_2, and the organic layer was dried over K_2CO_3. Flash chromatography using triethylamine/MeOH/CH_2Cl_2 (2:2:96) provided 800 mg (80%) of white solid [^{1}H NMR ($CDCl_3$): δ 7.30 (m, 5 H), 7.08 (d, 2 H), 6.81 (d, 2 H), 4.75 (m, 1 H), 4.58 (d, 1 H), 3.80 (m, 3 H), 2.75 (s, 3 H), 2.70 (m, 2 H), 2.43 (s, 1 H), 1.80 (m, 2 H), 1.07 (s, 9 H), 1.00 (d, 3 H), 0.26 (s, 6 H); there are also some minor rotomer peaks at 2.99 (s), 0.93 (d), and 0.22 (s)].

Homotyrosine. To a solution of 2.45 g of (−)-pseudoephedrine-4-*t*-butyldimethylsilyl-homotyrosinamide (5.37 mmol) in 10 ml of MeOH were added 25 ml of water and 16.5 ml of 1 N NaOH (16.5 mmol, 3 equivalents). The mixture was refluxed for 4 hr, and thin layer chromatography showed complete hydrolysis. Extraction with 2 × 25 ml of CH_2Cl_2 provided an aqueous solution of homotyrosine. The aqueous phase was then lyophilized to give 2.7 g of white solid. Because of the excess NaOH used and water trapped in the solid, the yield was higher than the theoretical yield of 1.28 g. The product was used directly for the next step [^{1}H NMR (D_2O): δ 6.97 (d, J = 8.6 Hz, 2 H), 6.53 (d, J = 8.6 Hz, 2 H), 3.22 (t, 1 H), 2.44 (t, 2 H), 1.78 (m, 2 H)].

NVOC-homotyrosine methyl ester. Into a solution of 600 mg of homotyrosine salt (1.19 mmol) in 50 ml of MeOH, gaseous HCl was bubbled for 10 min, which resulted in a light yellow solution. The mixture was then refluxed for 5 hr. The volatile compounds were removed by rotary-evaporation. The solid was used directly in the next step, by being dissolved in 10 ml of water with 252 mg of Na_2CO_3 (2.38 mmol, 2 equivalents). The resulting solution was then added in one portion to a solution of 328 mg of NVOC-Cl (1.19 mmol, 1 equivalent) in 10 ml of dioxane. The reaction mixture was kept for 30 min, acidified with 20 ml of 1 M KH_2PO_4, and extracted with 3 × 30 ml of CH_2Cl_2. The combined organic layer was dried over Na_2SO_4. Flash chromatography using ethyl acetate/petroleum ether (50:50) provided 330 mg (62% for two steps) of solid [^{1}H NMR ($CDCl_3$): δ 7.68 (s, 1 H), 6.99 (d, J = 8.0 Hz, 2 H), 6.95 (s, 1 H), 6.75 (d, J = 8.0 Hz, 2 H), 5.65 (d, J = 8.7 Hz, 1 H), 5.57 (d, J = 15.1 Hz, 1 H), 5.45 (d, J = 15.1 Hz, 1 H), 4.37 (m, 1 H), 3.97 (s, 3 H), 3.92 (s, 3 H), 3.68 (s, 3 H), 2.60 (t, 2 H), 2.10 (m, 1 H), 1.94 (m, 1 H)].

NVOC-4-nitroveratryl-homotyrosine methyl ester. To a solution of 290 mg of NVOC-homotyrosine methyl ester (0.647 mmol) in 40 ml of dry acetonitrile were added 98 mg of K_2CO_3 (0.712 mmol, 1.1 equivalents) and 165 mg of nitroveratryl chloride (0.712 mmol, 1.1 equivalents). The mixture was refluxed overnight. The volatile compounds were then removed by rotary-evaporation. Flash chromatography using ethyl acetate/petroleum ether (60:40) provided 350 mg (84%) of solid [^{1}H NMR ($CDCl_3$): δ 7.80 (s, 1 H), 7.74 (s, 1 H), 7.37 (s, 1 H), 7.13 (d, J = 9.0 Hz, 2 H), 7.03 (s, 1 H), 6.94 (d, J = 9.0 Hz, 2 H), 5.50 (m, 5 H), 4.44 (m, 1 H), 4.03 (s, 3 H), 4.01 (s, 3 H), 3.99 (s, 3 H), 3.98 (s, 3 H), 3.74 (s, 3 H), 2.69 (t, 2 H), 2.20 (m, 1 H), 2.00 (m, 1 H)].

NVOC-4-nitroveratryl-homotyrosine cyanomethyl ester. To a solution of 330 mg of NVOC-4-nitroveratryl-homotyrosine methyl ester (0.513 mmol) in 10 ml of CH_2Cl_2 were added 10 ml of 1 N NaOH and 10 drops of Aliquat 336. The reaction mixture was stirred vigorously at room temperature for 7 hr. The reaction was stopped and the two layers were separated. The aqueous layer was extracted once with 15 ml of CH_2Cl_2. The combined organic layer was dried over Na_2SO_4. Flash chromatography using ethyl acetate/petroleum ether/acetic acid (50:50:2) yielded the acid, which was used directly in the next step. The acid was dissolved in 1 ml of DMF, and 0.2 ml of chloroacetonitrile (3.16 mmol, 6 equivalents) and 0.2 ml of diisopropylethylamine (1.15 mmol, 2.24 equivalents) were added. The reaction mixture was kept in the dark overnight, diluted with 40 ml of ethyl acetate, and washed with 2 × 40 ml of KH_2PO_4 (1 M). The organic layer was dried over Na_2SO_4. Flash chromatography using ethyl acetate/petroleum ether (50:50) provided 300 mg (87% for two steps) of oily material [^{1}H NMR ($CDCl_3$): δ 7.78 (s, 1 H), 7.73 (s, 1 H), 7.35 (s, 1 H), 7.13 (d, J = 8.2 Hz, 2 H), 7.01 (s, 1 H), 6.95 (d, J = 8.2 Hz, 2 H), 5.56 (m, 5 H), 4.79 (d, J = 16.4 Hz, 1 H), 4.67 (d, J = 16.4 Hz, 1 H), 4.45 (m, 1 H), 4.02 (s, 3 H), 3.99 (s, 3 H), 3.98 (s, 3 H), 3.95 (s, 3 H), 2.69 (t, 2 H), 2.20 (m, 1 H), 2.08 (m, 1 H)].

dCA-NVOC-4-nitroveratryl-homotyrosine. This compound was prepared by the ligation procedure described above [FAB-MS: M^+ m/z 1247; calculated for $C_{48}H_{55}N_{11}O_{25}P_2$, 1247].

Results

Effects on EC_{50} for ACh

General issues. Table 1 summarizes the results of placing as many as 16 aromatic residues (14 unnatural residues plus tyrosine and phenylalanine) at positions 93, 190, and 198 in the α subunit of the nAChR. In each case the wild-type residue is tyrosine. The structures of the unnatural amino acids are given in Fig. 1. Clearly a wide range of derivatives of phenylalanine/tyrosine are compatible with the suppression system, giving measurable currents at one or more of the positions.

Our data consist of EC_{50} values as indicators of perturbations to the binding site. Of course, the EC_{50} involves contributions from both binding and gating, and there is evidence that one or more of the tyrosine residues studied here contributes to both (14, 15). For values near the wild-type value (49 μM), quite reliable and reproducible results were obtained. For example, we have three examples of rescue of wild-type activity using the suppression methodology (i.e., delivery of tyrosine as the "unnatural" residue). We obtained EC_{50} values of 49 μM at each of α93, α190, and α198. In general, we assigned an uncertainty of 3% to EC_{50} values of ≤100 μM. For higher EC_{50} values, there were additional systematic errors resulting from channel blockade by agonist, which distort and limit dose-response relations. Based on experience with the reproducibility of such cases and the necessarily truncated dose-response curves involved, we as-

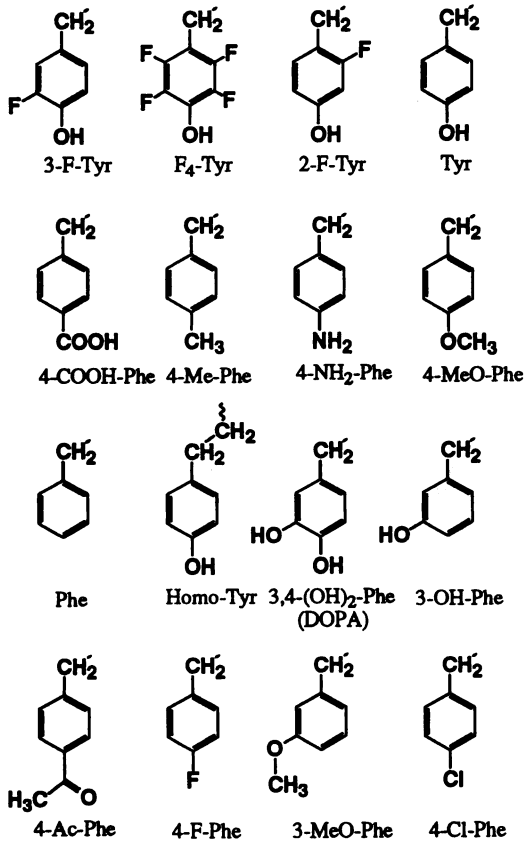

Fig. 1. Side-chain structures for the amino acids considered here. The residues are arranged in order of increasing EC_{50} for the α93 site (Table 1). *Me*, methyl; *MeO*, methoxy; *Ac*, acetyl.

signed uncertainties of 10% to EC_{50} values of 100–200 μM and 20% to values of 200–400 μM. We avoided extensive interpretation of experiments giving EC_{50} values of >400 μM.

Position α93. A very clear trend emerged from the data on the α93 site. With one exception, the data all fell into one of two categories, i.e., those with EC_{50} values essentially equal to the wild-type value and those with EC_{50} values >7 times greater than the wild-type value. There was also a clear structural correlation between the two categories. Those with nearly wild-type EC_{50} values (Fig. 1, *top row*) have a hydroxyl group in the 4-position, as in the wild-type tyrosine; those with very high EC_{50} values do not. The one apparent exception is DOPA, which has hydroxyl groups in both the 3- and 4-positions. It seems plausible that the interactions between these two adjacent hydroxyl groups interferes with the crucial role of the hydroxyl group in the 4-position.

Clearly, these data establish an especially prominent role for the hydroxyl group of Tyr93. Of course, the phenylalanine mutant shows that the hydroxyl group contributes in the wild-type tyrosine, but an especially informative unnatural amino acid is 4-methoxyphenylalanine. One possible difference between phenylalanine and tyrosine is the electronic perturbation of the aromatic ring expected from the hydroxyl group of tyrosine. The exact nature of such a perturbation depends on the context; phenol can be as much as 10^4 times more reactive than benzene in typical electrophilic aromatic substitutions, but the two are essentially equivalent in cation-π interactions (26, 27). However, in all contexts (reactivity toward electrophiles, π basicity, cation-π interactions, excited state energy, etc.) the electronic environment of the aromatic ring of 4-methoxyphenylalanine is nearly identical to that of tyrosine. Thus, the large difference between tyrosine and 4-methoxyphenylalanine proves that the π electronic structure of the aromatic ring is not the distinguishing feature between tyrosine and phenylalanine at α93. Rather, all of the evidence suggests that the hydrogen of the hydroxyl group is critical. One possibility, of course, is that Tyr93 is involved in an important hydrogen bond via the ring hydroxyl group (see below).

Position α190. Relatively little information about α190 can be gained from these studies. Of nine substitutions attempted, only five gave functional channels, and all of these (including phenylalanine) gave EC_{50} values >10-fold greater than the wild-type value. These include residues that give nearly wild-type responses at α93 and α198.

A negative result in these studies can mean a number of things. We know that all of the unnatural amino acids considered here are compatible with the *X. laevis* translational machinery, because they are incorporated at other sites of the receptor. A negative result could thus indicate that no intact receptors are ultimately formed (because of failure in folding, processing, transport to the membrane, or assembly) or that the receptors are formed but are not functional. We have not distinguished between these two possibilities.

We conclude that position α190 of the nAChR is an especially delicate site. Any change from the wild-type tyrosine either produces large changes in EC_{50} values or leads to no observable receptors. It thus seems likely that this residue fulfills some critical structural and/or functional role.

Position α198. As shown in Table 1, a large number of aromatic side chains can be introduced at α198. There are considerable variations in EC_{50} values in response to structural modifications and, although no simple pattern as in α93 is evident for α198, some general conclusions can be reached.

A conclusion that is perhaps obvious but is important is that α198 responds to structural changes very much differently than α93. For example, the best residue after wild-type tyrosine, even better than phenylalanine, is 4-methoxyphenylalanine. At α93 this residue falls into the high EC_{50} category, because it lacks a hydroxyl group. Clearly, the hydroxyl group is not critical at α198, and the hydroxyl group of the wild-type tyrosine is apparently not involved as a hydrogen bond donor. Thus, the unnatural amino acid methodology can clearly establish that two tyrosine residues in the same region of a receptor, both involved in agonist binding, are in quite different microenvironments structurally, in a way that conventional mutagenesis could not.

There are some general trends in the data for α198. It appears that a substituent in the 4-position is generally advantageous. Simple substituents like hydroxyl (all tyrosine derivatives), chlorine, fluorine, methyl, and methoxy all produce EC_{50} values below that of phenylalanine, suggesting that the 4-substituent at α198 is more a steric placeholder than a functional contributor to the receptor structure. Larger substituents such as acetyl and carboxylic acid groups are not as well tolerated. Increasing the overall size of the side chain (homotyrosine) or having any sizable substituent in the 3-position (3-methoxyphenylalanine, DOPA, and 3-hydroxyphenylalanine) is deleterious (fluorine is considered sterically undemanding). Of the 16 residues evaluated (14 unnatural residues plus tyrosine and phenylalanine), the

results for two are perhaps puzzling. As at α93, 4-aminophenylalanine activity is poor, and the high EC_{50} for 2-fluorotyrosine is unexplained.

Evaluation of Other Agonists (TMA and Nicotine)

Use of 9′-position mutants for low affinity agonists. We have conducted a survey of the effects of unnatural amino acids on two alternative agonists, i.e., TMA and nicotine. The former drug was chosen for its simple structure, the latter for its major differences from the structure of ACh itself. However, before presenting the results from these agonists, we describe a methodological advance that enables such studies.

Although TMA and nicotine are interesting because of their relatively simple structures, they also display EC_{50} values substantially greater than that of ACh for the wild-type receptor. Mutations would be expected to lead to further increases in EC_{50}, producing a situation in which very high concentrations of agonist are necessary. This can lead to complications such as channel blockade by the cationic agonists. To avoid such complications, we made use of observations concerning the effects of mutations in the M2 (channel-lining) region of the nAChR. For simplicity, we use the numbering system introduced previously, in which the amino terminus of the M2 domain is numbered as 1′ (28).

In particular, it has been established that leucine to serine mutations at the highly conserved 9′-position in the M2 region lead to marked decreases in EC_{50} (7, 29, 30). Further decreases can be obtained by combining M2 region L9′S mutations in multiple subunits (7, 30). The 9′-site is quite remote from the agonist binding site (31, 32), and we anticipated that the use of L9′S mutants would allow us to bring agonist EC_{50} values into an acceptable range without directly influencing the characteristics of the agonist binding site.

For studies of the α93 site, we used the βL9′S,γL9′S double-mutant; for the α198 site we employed the $(\alpha L9'S)_2$ double-mutant. Fig. 2 presents data showing that the $(\alpha L9'S)_2$ double-mutant has the constant effect of decreasing EC_{50} values by approximately 70-fold for several mutations at the α198 position. Similarly, the βL9′S,γL9′S double-mutant decreases EC_{50} by approximately 170-fold for three mutations at the α93 position. Thus, trends in the agonist binding site mutation data are not altered by introducing the various L9′S mutations. To a good approximation, the L9′S mutations simply shift the EC_{50} to a lower concentration. As additional support for the notion that the L9′S mutations do not seriously alter the agonist binding site, we can compare the two different L9′S double-mutants (α_2 versus $\beta\gamma$) with differing agonists. The ratio ([EC_{50} with $(\alpha L9'S)_2$]/[EC_{50} with βL9′S,γL9′S]) should be the same, regardless of the agonist. Using a wild-type agonist binding site, we find that this ratio is reasonably constant, i.e., 2.7, 4.0, and 3.1 for ACh, TMA, and nicotine, respectively. These ratios also agree with the study by Labarca *et al.* (7), which was performed with different vectors and much lower expression levels and yielded a similar ratio of 4.06 for ACh. Thus, to a good approximation, the 9′-position mutations have a consistent effect on EC_{50}, independent of agonist, and so the use of these mutant receptors to study weaker agonists is justified.

ACh versus TMA versus nicotine. Table 2 summarizes the results for the differing agonists with several mutations at α93 and α198. Considering ACh first, the trends across the series of unnatural residues at both α93 and α198 parallel the results previously reported for the receptor without the L9′S mutations. Interestingly, 3-fluorotyrosine at α93 again gives an EC_{50} below the wild-type value, confirming the observation with the 3-fluorotyrosine residue in the receptor with no mutations at the 9′-position (Table 1).

Fig. 3 shows that EC_{50} values remain proportional among ACh, nicotine, and TMA across a series of mutations in the agonist binding site. When plotted in logarithmic-logarithmic form to emphasize free-energy relationships, linear plots with slopes near 1 are observed. Especially telling is the excellent correlation between TMA and nicotine, two agonists with very different chemical structures. The largest deviation from linearity (ACh with 4-methoxyphenylalanine at α93) corresponds to a factor of 2.4 in EC_{50}. Although this is outside the expected error range for these measurements, attaching any physical significance to such a deviation would be difficult. We thus conclude that, as far as can be revealed

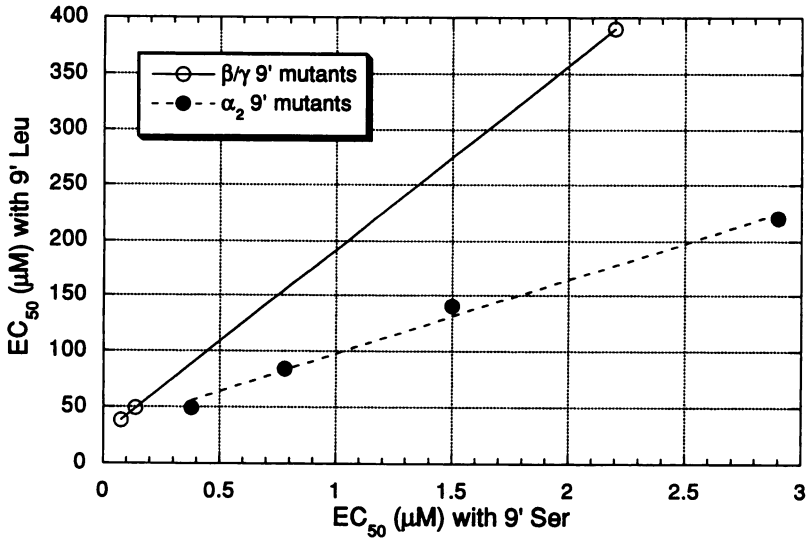

Fig. 2. Effect of L9′S mutations on EC_{50} values for ACh with various mutations in the agonist binding site. The β/γ L9′S mutants were evaluated with mutations at α93, and the α_2 L9′S mutants were evaluated with α198 mutants. Data are from Tables 1 and 2, with the latter defining the structures used.

TABLE 2
EC_{50} values for three agonists at receptors with L9'S mutations

Site	EC_{50}		
	ACh	TMA	Nicotine
		μM	
α93[a]			
Tyr	0.14	21	8.8
3-F-Tyr	0.077	14	7
4-MeO-Phe[b]	2.2	190	52
α198[c]			
Tyr	0.38	83	27
4-MeO-Phe	0.78	140	50
Phe	2.9	410	140
4-F-Phe	1.5	360	130

[a] βL9'S,γL9'S mutants.
[b] MeO, methoxy.
[c] $(\alpha L9'S)_2$ mutants.

by this limited study, ACh, nicotine, and TMA do not interact in dramatically different ways with either α93 or α198.

Discussion

General Conclusions

The present study represents the first full report on the stop codon suppression methodology in combination with the heterologous expression system of *X. laevis* oocytes. The data show that this technique can be used to incorporate a large number of unnatural amino acids at functionally important sites of an ion channel protein such as the nAChR. The broad tolerance of the *in vivo* translational machinery augers well for future studies involving unnatural amino acids that are more dramatically different from the naturally occurring residues. An additional advantage of the suppressor methodology is that, once the UAG mutation is placed at the codon of interest, it is a fairly simple matter to introduce a wide range of substituents. That is, each EC_{50} value from Table 1 does not represent a new round of mutagenesis. One simply injects a different aminoacyl-tRNA to obtain a new residue at the position of interest. This makes it a much simpler matter to survey a wide range of substitutions, including the natural amino acids, which are efficiently incorporated by this methodology.

The results described here confirm and extend earlier experiments (1, 12–15) based on both conventional and unnatural mutagenesis, which suggested differing roles for the remarkable array of aromatic residues thought to be involved in defining the agonist binding site of the nAChR. We have considered three sites for which tyrosine is highly conserved in wild-type receptors and for which conventional tyrosine to phenylalanine mutagenesis gives qualitatively similar results. Studying a series of unnatural amino acids, however, reveals clear distinctions among these residues.

This paper also presents the first study on simultaneous variations in the structures of receptor side chains and agonists. The goal was to produce decisive quantitative data about interactions between moieties in the agonist and in the side chains at the binding site. The data are sufficiently quantitative to yield a simple conclusion, namely, we find little evidence for specific distinctions among the agonists.

An additional methodological advance, which also has significant implications for the mode of action of the nAChR, is described by our observations that M2 region 9'-position mutations change EC_{50} values by factors that, to a first-order approximation, do not depend on the nature of the agonist or mutations at the binding site. That is, both the agonist binding site, associated primarily with the extracellular amino-terminal domain of the α subunit, and the M2 domain of each subunit contribute to channel activation. However, the two regions are in one sense independent, in that changes at the M2 region 9'-position do not substantially alter the energetic consequences of structural modifications at the binding site, and vice versa.

Side-Chain Structural Influences on EC_{50}

Position α93. At α93 a prominent role for the tyrosine hydroxyl group is established, as suggested from less extensive data obtained in an earlier study (1) and studies with conventional mutagenesis (12–15). However, closer scrutiny reveals a more subtle effect. The four structures with nearly wild-type EC_{50} values are known to have quite different pK_a values for the aromatic hydroxyl group. The best estimates are 10, 9.3, 8.8, and 5.3 for tyrosine, 2-fluorotyrosine, 3-fluorotyrosine, and tetrafluorotyrosine, respectively (31). This means that, at physiological pH, the hydroxyl group of tetrafluorotyrosine should be ionized to an anionic phenolate but the hydroxyl group of tyrosine should not. We consider it completely implausible that two residues, one an anion and the other a neutral group, should produce essentially identical EC_{50} values for the cationic agonist ACh. Given the data of Table 1, we conclude that all of the residues with EC_{50} values near the wild-type value are in the same ionization state. Of course, the above arguments concerning pK_a values are for groups that are freely exposed to an aqueous environment, and evidently this is not the case for α93 of the nAChR.

There are numerous examples of anomalous pK_a values for residues in proteins. The simplest mechanism is to place the side chain in a generally hydrophobic environment that is not well exposed to water. Under these conditions, pK_a values are elevated, and it is completely plausible that the fluorinated tyrosines would not be ionized to any significant extent. Given the large number of hydrophobic residues known to be near the agonist binding site, it is not unreasonable to propose a hydrophobic environment for the hydroxyl group of αTyr93.

Another way to alter the apparent pK_a of a hydroxyl group is to involve it in a hydrogen bond. In fact, a recent study of a tyrosine that is hydrogen-bonded to a glutamate in staphylococcal nuclease established that the hydrogen bond persists when the tyrosine is replace by tetrafluorotyrosine (33). Qualitatively, our results are consistent with the involvement of Tyr93 in a hydrogen bond. The strong distinction between tyrosine and 4-methoxyphenylalanine supports this view. Also, the fact that 4-aminophenylalanine is in the "no hydrogen bond" category is consistent with the well recognized fact that aromatic amines (anilines) are much poorer hydrogen-bond donors than are phenols (34). However, it is generally true that hydrogen bond strengths correlate with the acidity of the donor. For example, the recent study of staphylococcal nuclease mentioned above showed a linear free-energy relationship between unfolding energy and the pK_a values of the four side chains under consideration here (33). We do not see a similar quantitative correlation between the pK_a of the hydroxyl group and EC_{50}. There are slight variations that are, at best, barely significant. It is intriguing

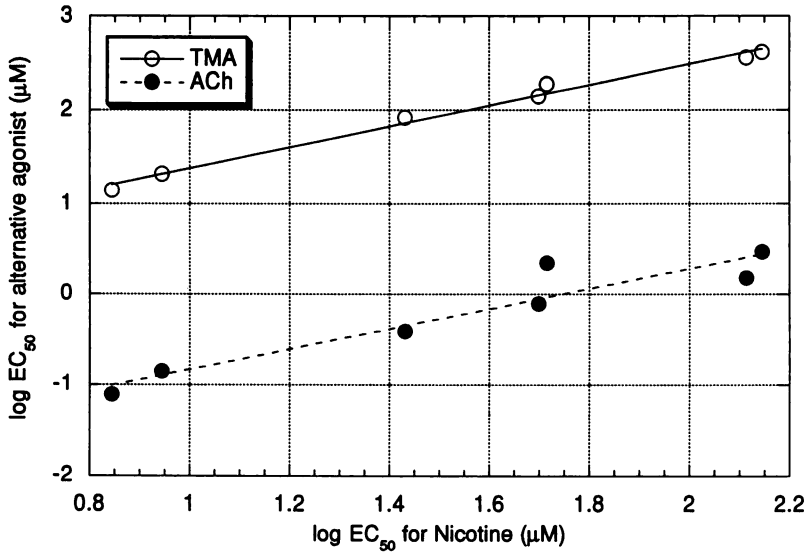

Fig. 3. Relationships among EC_{50} values for the three agonists and the various mutations studied here. *Lines*, linear least-squares fits; both have a slope of 1.1. Data are from Table 2.

that 2-fluorotyrosine and 3-fluorotyrosine both show EC_{50} values below the wild-type value, and for these two plus tyrosine the values do roughly correlate with pK_a. For tetrafluorotyrosine, the EC_{50} is slightly below the wild-type value, but not as much as expected from its pK_a. These changes are too small to interpret with confidence, but they are suggestive. Of course, EC_{50} is a more complicated indicator of protein structure than is unfolding energy, because it involves contributions from both binding and gating. It could be that in the nAChR there are compensating effects that mask any simple free-energy relationship.

A third possibility, which we consider to be the least likely, is that all hydroxyl-containing residues are in fact ionized, and it is the presence of the negative charge that enhances ACh affinity. There is much less precedent for lowering pK_a values in proteins, and to our knowledge there is no unambiguous evidence for an ionized tyrosine in a protein.

The one unnatural amino acid that remains by itself at α93 is 4-carboxyphenylalanine, with a EC_{50} intermediate between those of the high and low groups. We interpret this as a structure that does have a hydroxyl group, but one that is not as optimally positioned as in the four tyrosine derivatives with wild-type EC_{50} values. In this light, its position as an "intermediate" residue is understandable. Note however, that the "natural" pK_a of 4-carboxyphenylalanine is approximately 4, which places even more demands on the environment if this residue, too, is to be considered unionized. If this argument is correct, then the requisite positioning of the hydroxyl group must be fairly delicate, because an alternative repositioning, as represented by 3-hydroxyphenylalanine, produces a very high EC_{50}.

Positions α190 and α198. The tyrosine at α190 appears to be in an especially critical position, inasmuch as all mutations lead to either greatly elevated EC_{50} values or detection of no functional receptors. This observation fits well with suggestions (14, 15) that position 190 is involved in both agonist binding and the conformational change that governs gating. In contrast, position α198 is quite tolerant to substitution, and we have characterized 15 mutants plus the wild-type tyrosine at this site. In sharp contrast to α93, no special role is seen for the hydroxyl group of αTyr198. This is clearly established by the observation that 4-methoxyphenylalanine gives nearly wild-type behavior at this position.

Concerning the cation-π site. None of the three tyrosine residues evaluated here produces an EC_{50} pattern in response to substitution that is strongly suggestive of the side chain being involved in cation-π interactions. This is perhaps not surprising, because tryptophan is the critical cation-π residue at both the active site and the "peripheral anionic site" of the ACh esterase (8, 9), as well as for the quaternary ammonium ion recognition by the McPC603 phosphocholine-binding Fab (10, 35). In addition, recent theoretical studies (26, 27) establish that the indole side chain of tryptophan is superior to the phenol side chain of tyrosine in cation-π binding. It seems likely that one or more of the highly conserved tryptophan residues of the nAChR agonist binding site is involved in cation-π interactions.

Comparisons Among Three Agonists

We used M2 region 9′-position serine mutations to enable studies of agonist/mutation combinations that would be too weak for quantitative study if the wild-type leucine were present at the M2 region 9′-position. We studied variations in EC_{50} produced by the unnatural residues at positions α93 and α198, two residues now established to be in significantly different structural microenvironments. The agonists ACh, TMA, and nicotine, which share only the cationic ammonium group as a common structural feature, were considered. Each agonist leads to a roughly 30-fold range in EC_{50}. All three display the same rank order of EC_{50} values and, in fact, lead to roughly proportional EC_{50} values over the entire range (Fig. 3). Apparently, the interactions of all three agonists with α93 and α198 are similar, whether they involve direct contact with the side chain or indirect interactions mediated by other residues. From these observations it is clear that, at least in the present system, the tactic of varying agonist structure is a relatively insensitive probe of differing structural microenvironments at a binding site, compared with the unnatural amino acid methodology.

The problem of agonist-receptor interactions in the nAChR

and related structures is still in great need of atomic-scale structural information. Until X-ray crystallography and NMR spectroscopy become generally applicable to these integral membrane proteins, the combination of unnatural amino acid mutagenesis and high-resolution electrophysiology has the potential to provide the most detailed structure-function data for neuroreceptors. The present work establishes the broad applicability of this methodology, especially when combined with other techniques, such as conventional mutagenesis and pharmacological analyses (agonist variation).

Acknowledgments

We thank Dr. Margaret E. Saks and Dr. Jeffrey R. Sampson for providing T7 polymerase and helpful advice.

References

1. Nowak, M. W., P. C. Kearney, J. R. Sampson, M. E. Saks, C. G. Labarca, S. K. Silverman, W. Zhong, J. Thorson, J. N. Abelson, N. Davidson, P. G. Schultz, D. A. Dougherty, and H. A. Lester. Nicotinic receptor binding site probed with unnatural amino-acid incorporation in intact cells. *Science (Wash. D. C.)* **268**:439–442 (1995).
2. Noren, C. J., S. J. Anthony-Cahill, M. C. Griffith, and P. G. Schultz. A general method for site-specific incorporation of unnatural amino acids into proteins. *Science (Wash. D. C.)* **244**:182–188 (1989).
3. Cornish, V. W., D. Mendel, and P. G. Schultz. Probing protein structure and function with an expanded genetic code. *Angew. Chem. Int. Ed. Engl.* **34**:621–633 (1995).
4. Karlin, A. Structure of nicotinic acetylcholine receptors. *Curr. Opin. Neurobiol.* **3**:299–309 (1993).
5. Devillers-Thiéry, A., J. L. Galzi, J. L. Eiselé, S. Bertrand, D. Bertrand, and J. P. Changeux. Functional architecture of the nicotinic acetylcholine receptor: a prototype of ligand-gated ion channels. *J. Membr. Biol.* **136**: 97–112 (1993).
6. Lester, H. A. The permeation pathway of neurotransmitter-gated ion channels. *Annu. Rev. Biophys. Biomol. Struct.* **21**:267–292 (1992).
7. Labarca, C., M. W. Nowak, H. Zhang, L. Tang, P. Deshpande, and H. A. Lester. Channel gating governed symmetrically by conserved leucine residues in the M2 domain of nicotinic receptors. *Nature (Lond.)* **376**:514–516 (1995).
8. Sussman, J. L., M. Harel, F. Frolow, C. Oefner, A. Goldman, L. Toker, and I. Silman. Atomic structure of acetylcholinesterase from *Torpedo californica*: a prototypic acetylcholine-binding protein. *Science (Wash. D. C.)* **253**:872–879 (1991).
9. Silman, I., M. Harel, P. Axelsen, M. Raves, and J. L. Sussman. Three-dimensional structures of acetylcholinesterase and of its complexes with anticholinesterase agents. *Biochem. Soc. Trans.* **22**:745–749 (1994).
10. Dougherty, D. A., and D. A. Stauffer. Acetylcholine binding by a synthetic receptor: implications for biological recognition. *Science (Wash. D. C.)* **250**:1558–1560 (1990).
11. Dougherty, D. A. Cation-π interactions in chemistry and biology: a new view of benzene, Phe, Tyr, and Trp. *Science (Wash. D. C.)* **271**:163–168 (1996).
12. Tomaselli, G. F., J. T. McLaughlin, M. E. Jurman, E. Hawrot, and G. Yellen. Mutations affecting agonist sensitivity of the nicotinic acetylcholine receptor. *Biophys. J.* **60**:721–727 (1991).
13. Aylwin, M. L., and M. M. White. Ligand-receptor interactions in the nicotinic acetylcholine receptor probed using multiple substitutions at conserved tyrosines on the α subunit. *FEBS Lett.* **349**:99–103 (1994).
14. Chen, J., Y. Zhang, G. Akk, S. Sine, and A. Auerbach. Activation kinetics of recombinant mouse nicotinic acetylcholine receptors: mutations of α-subunit tyrosine 190 affect both binding and gating. *Biophys. J.* **69**:849–859 (1995).
15. Sine, S. M., P. Quiram, F. Papanikolaou, H.-J. Kreienkamp, and P. Taylor. Conserved tyrosines in the α subunit of the nicotinic acetylcholine receptor stabilize quaternary ammonium groups of agonists and curariform antagonists. *J. Biol. Chem.* **269**:8808–8816 (1994).
16. Grodberg, J., and J. J. Dunn. *ompT* encodes the *Escherichia coli* outer membrane protease that cleaves T7 RNA polymerase during purification. *J. Bacteriol.* **170**:1245–1253 (1988).
17. Davanloo, P., A. H. Rosenberg, J. J. Dunn, and F. W. Studier. Cloning and expression of the gene for bacteriophage T7 RNA polymerase. *Proc. Natl. Acad. Sci. USA* **81**:2035–2039 (1984).
18. Saks, M. E., J. R. Sampson, M. W. Nowak, P. C. Kearney, F. Du, J. N. Abelson, H. A. Lester, and D. A. Dougherty. An engineered *tetrahymena* $tRNA^{Gln}$ for *in vivo* incorporation of unnatural amino acids into proteins by nonsense suppression. *J. Biol. Chem.* **271**:23169–23175 (1996).
19. Sampson, J. R., and O. C. Uhlenbeck. Biochemical and physical characterization of an unmodified yeast phenylalanine transfer RNA transcribed *in vitro*. *Proc. Natl. Acad. Sci. USA* **85**:1033–1037 (1988).
20. Quick, M. W., and H. A. Lester. Methods for the expression of excitability proteins in *Xenopus* oocytes, in *Ion Channels of Excitable Cells* (T. Narahashi, ed.). Academic Press, San Diego, 261–279 (1994).
21. England, T. E., A. G. Bruce, and O. C. Uhlenbeck. Specific labeling of 3′ termini of RNA with T4 RNA ligase. *Methods Enzymol.* **65**:65–74 (1980).
22. Ellman, J., D. Mendel, S. Anthonycahill, C. J. Noren, and P. G. Schultz. Biosynthetic method for introducing unnatural amino-acids site-specifically into proteins. *Methods Enzymol.* **202**:301–336 (1991).
23. Knittel, J. J., and X. He. Synthesis and resolution of novel 3′-substituted phenylalanine amides. *Pept. Res.* **3**:176–181 (1990).
24. Cabri, W., I. Candiani, A. Bedeschi, S. Penco, and R. Santi. *Alpha*-regioselectivity in palladium-catalyzed arylation of acyclic enol ethers. *J. Org. Chem.* **57**:1481–1486 (1992).
25. Myers, A. G., J. L. Gleason, and T. Y. Yoon. A practical method for the synthesis of D-*alpha*-amino or L-*alpha*-amino acids by the alkylation of (+)-pseudoephedrine or (−)-pseudoephedrine glycinamide. *J. Am. Chem. Soc.* **117**:8488–8489 (1995).
26. Mecozzi, S., A. P. West, Jr., and D. A. Dougherty. Cation-π interactions in simple aromatics: electrostatics provide a predictive tool. *J. Am. Chem. Soc.* **118**:2307–2308 (1996).
27. Mecozzi, S., A. P. West, Jr., and D. A. Dougherty. Cation-π interactions in aromatics of biological and medicinal interest: electrostatic potential surfaces as a useful qualitative guide. *Proc. Natl. Acad. Sci. USA* **93**:10566–10571 (1996).
28. Charnet, P., C. Labarca, R. J. Leonard, N. J. Vogelaar, L. Czyzyk, A. Gouin, N. Davidson, and H. A. Lester. An open-channel blocker interacts with adjacent turns of α-helices in the nicotinic acetylcholine receptor. *Neuron* **2**:87–95 (1990).
29. Revah, F., D. Bertrand, J.-L. Galzi, A. Devillers-Thiéry, C. Mulle, N. Hussy, S. Bertrand, M. Ballivet, and J.-P. Changeux. Mutations in the channel domain alter desensitization of a neuronal nicotinic receptor. *Nature (Lond.)* **353**:846–849 (1991).
30. Filatov, G. N., and M. M. White. The role of conserved leucines in the M2 domain of the acetylcholine receptor in channel gating. *Mol. Pharmacol.* **48**:379–384 (1995).
31. Unwin, N. Nicotinic acetylcholine receptor at 9 Å resolution. *J. Mol. Biol.* **229**:1101–1124 (1993).
32. Unwin, N. Acetylcholine receptor channel imaged in the open state. *Nature (Lond.)* **373**:37–43 (1995).
33. Thorson, J. S., E. Chapman, E. C. Murphy, P. G. Schultz, and J. K. Judice. Linear free energy analysis of hydrogen bonding in proteins. *J. Am. Chem. Soc.* **117**:1157–1158 (1995).
34. Thorson, J. S., E. Chapman, and P. G. Schultz. Analysis of hydrogen bonding strengths in proteins using unnatural amino acids. *J. Am. Chem. Soc.* **117**:9361–9362 (1995).
35. Satow, Y., G. H. Cohen, E. A. Padlan, and D. R. Davies. Phosphocholine-binding immunoglobulin Fab McPC603. *J. Mol. Biol.* **190**:593–604 (1986).

Send reprint requests to: Dr. D. A. Dougherty, Division of Chemistry and Chemical Engineering, Mail Code 164–30, California Institute of Technology, Pasadena, CA 91125. E-mail: dad@igor.caltech.edu